

THE DISTRIBUTION AND COSMIC EVOLUTION OF MASSIVE BLACK HOLE SPINS

MARTA VOLONTERI¹, PIERO MADAU¹, ELIOT QUATAERT², & MARTIN J. REES³

ApJ, in press

ABSTRACT

We study the expected distribution of massive black hole (MBH) spins and its evolution with cosmic time in the context of hierarchical galaxy formation theories. Our model uses Monte Carlo realizations of the merger hierarchy in a Λ CDM cosmology, coupled to semi-analytical recipes, to follow the merger history of dark matter halos, the dynamics of the MBHs they host, and their growth via gas accretion and binary coalescences. The coalescence of comparable mass holes increases the spin of MBHs, while the capture of smaller companions in randomly-oriented orbits acts to spin holes down. We find that, given the distribution of MBH binary mass ratios in hierarchical models, binary coalescences alone do not lead to a systematic spin-up or spin-down of MBHs with time: the spin distribution retains memory of its initial conditions. By contrast, because of the alignment of a MBH with the angular momentum of the outer accretion disk, gas accretion tends to spin holes up even if the direction of the spin axis varies in time. In our models, accretion dominates over black hole captures and efficiently spins holes up. The spin distribution is heavily skewed towards fast-rotating Kerr holes, is already in place at early epochs, and does not change much below redshift 5. If accretion is via a thin disk, about 70% of all MBHs are maximally rotating and have radiative efficiencies approaching 30% (assuming a “standard” spin-efficiency conversion). Even in the conservative case where accretion is via a geometrically thick disk, about 80% of all MBHs have spin parameters $a/m_{\text{BH}} > 0.8$ and accretion efficiencies $> 12\%$. Rapidly spinning holes with high radiative efficiencies may satisfy constraints based on comparing the local MBH mass density with the mass density inferred from luminous quasars (Soltan’s argument). Since most holes rotate rapidly at all epochs, our results suggest that spin is not a necessary and sufficient condition for producing a radio-loud quasar.

Subject headings: black hole physics – cosmology: theory – galaxies: active – galaxies: nuclei – quasars: general

1. INTRODUCTION

Dynamical evidence indicates that massive black holes (MBHs) reside at the centers of most nearby galaxies (Richstone et al. 1998). The tight correlation observed between their masses and the stellar velocity dispersion or mass of the host bulge (Gebhardt et al. 2000; Ferrarese & Merritt 2000; Häring & Rix 2004) suggests a close relationship between the growth of black holes and spheroids in galaxy halos. It is not yet understood which physical processes established this correlation and how it is maintained through cosmic time with such a small dispersion.

Besides their masses, m_{BH} , astrophysical black holes are completely characterized by their spins, $S = aGm_{\text{BH}}/c$, $0 \leq a/m_{\text{BH}} \leq 1$. The spin of a MBH is expected to have a significant effect on its observational manifestation. For example, the spin determines the efficiency of converting accreted mass into radiation and has implications for the direction of jets in active nuclei (Rees 1984). The electromagnetic braking of a rapidly spinning black hole may extract rotational energy (Blandford & Znajek 1977), convert it into directed Poynting flux and electron-positron pairs, and power some radio galaxies and gamma-ray bursts. The orientation of the spin is thought to determine the innermost flow pattern of gas accreting onto Kerr holes (Bardeen & Petterson 1975). The coalescence of two

spinning black holes in a radio galaxy may cause a sudden reorientation of the jet direction, perhaps leading to the so-called “winged” or “X-type” radio sources (Merritt & Ekers 2002).

The spin of a MBH is determined by the competition between a number of physical processes. Black holes forming from the gravitational collapse of very massive stars endowed with rotation will in general be born with non-zero spin (e.g. Fryer, Woosley, & Heger 2002). An initially non-rotating hole that increases its mass by (say) 50% by swallowing material from an accretion disk may be spun up to $a/m_{\text{BH}} = 0.84$ (Bardeen 1970). While the coalescence of two non-spinning black holes of comparable mass will immediately drive the spin parameter of the merged hole to $a/m_{\text{BH}} \gtrsim 0.8$ (e.g. Gammie, Shapiro, & McKinney 2004), the capture of smaller companions in randomly-oriented orbits may spin down a Kerr hole instead (Hughes & Blandford 2003, hereafter HB).

In this paper we make a first attempt at estimating the distribution of MBH spins and its evolution with cosmic time in the context of hierarchical structure formation theories. In the next section we review the assembly of MBHs in popular cold dark matter (CDM) cosmogonies. We then address the evolution of MBH spin via coalescences (§3) and gas accretion (§4). We compute the spin distribution of MBHs in §5, and summarize our results and discuss

¹Department of Astronomy & Astrophysics, University of California, Santa Cruz, CA 95064; pmadau@ucolick.org, marta@ucolick.org.

²Department of Astronomy, 601 Campbell Hall, University of California at Berkeley, Berkeley, CA 94720; eliot@astron.berkeley.edu.

³Institute of Astronomy, Madingley Road, Cambridge CB3 0HA, UK; mjr@ast.cam.ac.uk.

their implications in §6.

2. ASSEMBLY AND GROWTH OF MBHs

The main features of a plausible scenario for the hierarchical assembly, growth, and dynamics of MBHs in a Λ CDM cosmology have been discussed in Volonteri, Haardt, & Madau (2003), and Volonteri, Madau, & Haardt (2003). Dark matter halos and their associated galaxies undergo many mergers as mass is assembled from high redshift to the present. The halo merger history is tracked backwards in time with a Monte Carlo algorithm based on the extended Press-Schechter formalism. “Seed” holes form with intermediate masses in the rare high- σ peaks (“minihalos”) collapsing at $z = 20 - 25$ (Madau & Rees 2001), and their growth and dynamical evolution is followed in detail with a semi-analytical technique. The merging – driven by dynamical friction against the dark matter – of two comparable-mass halo+MBH systems (“major mergers”) drags in the satellite hole towards the center of the more massive progenitor, leading to the formation of a bound MBH binary with separation of \sim pc. The long dynamical frictional timescales leave many MBHs “wandering” in galaxy halos after a merger between halos of large mass ratio (“minor mergers”).

A two-component model for galaxy halos is adopted, where the dark matter is distributed according to an NFW profile (Navarro, Frenk, & White 1997), while the initial central stellar distribution is a singular isothermal sphere with stellar velocity dispersion, σ_* . The latter is related to the halo circular velocity following Ferrarese (2002). The present-day mass density of nuclear MBHs accumulates via gas accretion: in every major merger, the heavier hole accretes at the Eddington rate a gas rest mass Δm_0 . This leads to a change in the total mass-energy of the hole given by

$$\Delta m = 3.6 \times 10^6 M_\odot V_{c,150}^{5.2}, \quad (1)$$

where $V_{c,150}$ is the circular velocity of the merged system in units of 150 km s^{-1} (Volonteri, Madau, & Haardt 2003). The scaling with the fifth power of the circular velocity of the host halo and the normalization are fixed in order to reproduce the observed local $m_{\text{BH}} - \sigma_*$ relation. The quantities Δm and Δm_0 are related by $\Delta m = (1 - \epsilon) \Delta m_0$, where ϵ is the mass-to-energy conversion efficiency, equal for thin-disk accretion to the binding energy per unit mass of a particle in the last stable circular orbit.⁴ This model was shown in Volonteri, Haardt, & Madau (2003) to reproduce well the observed luminosity function of optically-selected quasars in the redshift range $1 < z < 5$.

2.1. MBH binaries

The semimajor axis of a bound MBH binary continues to shrink owing to dynamical friction from distant stars acting on each hole individually, until the pair becomes “hard” when the separation falls below $a_h = Gm_2(4\sigma_*^2)$ (Quinlan 1996), where $m_2 (< m_1)$ is the mass of the lighter

hole. After this stage the MBH pair hardens via three-body interactions, i.e., by capturing and ejecting at much higher velocities the stars passing within a distance of order the binary separation (Begelman, Blandford, & Rees 1980). Our scheme assumes that the “bottleneck” stages of binary shrinking occur for separations smaller than a_h ; during a galactic merger, after a dynamical friction timescale, we place the MBH pair at a_h and let it evolve. The hardening of the binary modifies the stellar density profile, removing mass interior to the binary orbit, depleting the galaxy core of stars, and slowing down further hardening. The above scheme can be modified by rare triple black hole interactions, when another major merger takes place before the pre-existing binary has had time to coalesce (Saslaw, Valtonen, & Aarseth 1974). In this case there is a net energy exchange between the binary and the third incoming black hole, resulting in the ejection of the lighter hole and the recoil of the binary. The binary also becomes more tightly bound. Our scheme implicitly neglects the depopulation of the “loss cone,” i.e. it assumes a large supply of low-angular momentum stars (as one might expect in significantly flattened or triaxial galaxies, Yu 2002). It also neglects the role of gaseous – rather than stellar dynamical – processes in driving the evolution of a MBH binary (e.g. Escala et al. 2004; Armitage & Natarajan 2002).

If stellar dynamical and/or gas processes drive the binary sufficiently close ($\lesssim 0.01$ pc), gravitational radiation will eventually dominate angular momentum and energy losses and cause the two MBHs to coalesce.

3. SPIN CHANGE BY BINARY COALESCENCES

HB have recently addressed how binary coalescence changes the spin of the remnant hole. We follow here their treatment. The problem is simpler for small mass ratios, $q \equiv m_2/m_1 \ll 1$, as the binary is then well described by a test particle, the orbit of which shrinks due to gravitational wave emission to the last stable orbit (LSO): the smaller hole then plunges into the more massive one adding the LSO angular momentum to its spin (since a black hole spin scales with its mass squared, the small hole’s spin can be neglected). While the test particle description is not accurate for $q \gtrsim 0.5$, binary coalescences with mass ratios larger than 0.5 take place in only 10% of our simulations at $1 < z < 5$, and are even more rare at $z < 1$ (see Figure 1). Moreover, the test particle description is qualitatively correct in that $q \gtrsim 0.5$ coalescences lead to rapidly spinning holes most of the time (see Figs. 2 and 3).

We adopt below geometrized units and set $c = G = 1$; hatted quantities have been made dimensionless by dividing out powers of mass, e.g. $\hat{a}_1 \equiv a_1/m_1$. Before coalescence, the larger hole has mass m_1 and spin $|\mathbf{S}| = \hat{a}_1 m_1^2$. Kerr geodesics orbits are specified by choosing their energy E , angular momentum parallel to the spin, L_z , and “Carter constant” Q . Orbits with $Q \neq 0$ are inclined at angle θ with respect to the equatorial plane, $\cos \theta = L_z / \sqrt{L_z^2 + Q} \equiv \mu$.

⁴The conversion from black hole spin to radiative efficiency is still debated, and depends on whether or not magnetic stresses exert a significant torque at the last stable orbit (e.g. Krolik, Hawley, & Hirose 2004); here we adopt the standard definition for circular equatorial orbits around a Kerr hole. For prograde orbits, the mass-to-energy conversion efficiency $\epsilon \equiv 1 - \hat{E}$ can then be expressed as $\hat{a} = 2/(3\sqrt{3}) \left[2\sqrt{2/(2\epsilon - \epsilon^2)} - (1 - \epsilon)/(2\epsilon - \epsilon^2) \right]$.

The smaller hole plunges into the large one carrying along its orbital constants at the LSO⁵; given the inclination angle, one can determine the radius of the LSO, L_z , and E by numerically solving the system $R = \partial R / \partial r = \partial^2 R / \partial r^2 = 0$, where R is the “effective potential” governing radial motion. The constants are bounded by their values for prograde ($\mu = 1$) and retrograde ($\mu = -1$) equatorial orbits,

$$\hat{r} \equiv r_{\text{LSO}}/m_1 = 3 + Z_2 \mp \sqrt{(3 - Z_1)(3 + Z_1 + 2Z_2)}, \quad (2)$$

$$\hat{E} \equiv E_{\text{LSO}}/m_2 = \left(1 - \frac{2}{3\hat{r}}\right)^{1/2}, \quad (3)$$

$$\hat{L} \equiv L_{\text{LSO}}/(m_2 m_1) = \pm \frac{2}{3\sqrt{3}}[1 + 2(3\hat{r} - 2)^{1/2}], \quad (4)$$

$$\hat{Q} = 0, \quad (5)$$

where Z_1 and Z_2 are functions of \hat{a}_1 only (Bardeen, Press, & Teukolsky 1972), and the upper (lower) sign refers to prograde (retrograde) orbits. According to HB, the numerical results are remarkably well fitted by

$$\xi(\mu) \simeq |\xi_{\text{ret}}| + \frac{1}{2}(\mu + 1)(\xi_{\text{pro}} - |\xi_{\text{ret}}|), \quad (6)$$

where ξ stands for \hat{r} , \hat{E} , or \hat{L} , and the “ret” and “pro” subscripts correspond to retrograde and prograde orbits, respectively. After capturing the smaller hole, the remnant MBH has mass and spin given by

$$m' = m_1[1 + q\hat{E}(\hat{a}_1, \mu)], \quad (7)$$

$$S'_z = m_1^2[\hat{a}_1 + q\hat{L}_z(\hat{a}_1, \mu)], \quad (8)$$

$$S'_\perp = qm_1^2\hat{L}_z(\hat{a}_1, \mu)\sqrt{\mu^{-2} - 1}. \quad (9)$$

The remnant hole is inclined at an angle $\Delta\theta$ relative to the original hole, and has final spin parameter \hat{a}' :

$$\Delta\theta = \arccos\left(\frac{S'_z/\sqrt{S'^2_z + S'^2_\perp}}{S'_z/\sqrt{S'^2_z + S'^2_\perp}}\right), \quad (10)$$

$$\hat{a}' = \sqrt{S'^2_z + S'^2_\perp}/m'^2. \quad (11)$$

Figures 2 and 3 show how, following a single coalescence, the spin of the remnant hole \hat{a}' depends on the mass ratio and inclination cosine for two representative values of the initial spin \hat{a}_1 . There is little change in spin for $q < 0.05$, while for larger mass ratios the angular momentum \mathbf{L} at the LSO overwhelms the initial spin \mathbf{S} of the hole. For randomly-distributed inclination angles, MBHs that are initially rotating with $\hat{a}_1 = 0.6$ are spun up even further for $q > 0.125$, and are spun down otherwise. Rapidly rotating holes, with $\hat{a}_1 = 0.9$, are typically spun down except for large mass ratios and close-to-prograde orbits.

4. SPIN CHANGES BY ACCRETION

Accretion from a disk of gas orbiting the hole will cause the spin to evolve in both magnitude and orientation. If the disk is in the equatorial plane of a Kerr

hole, and gas is dumped directly down the hole from the LSO, then the accretion of a rest mass dm_0 will lead to a change $dm = \hat{E} dm_0$ in the total gravitational mass and $dS_z = \hat{L}_z m dm_0$ in the total angular momentum of the hole. The evolution of the hole spin is governed by the differential equation

$$\frac{d\hat{a}}{d \ln m} = \frac{\hat{L}_z}{\hat{E}} - 2\hat{a}. \quad (12)$$

This was integrated by Bardeen (1970) to obtain the evolution law

$$\hat{a}' = \frac{\hat{r}^{1/2} m_1}{3 m'} \left[4 - \left(\frac{3m_1^2}{m'^2} \hat{r} - 2 \right)^{1/2} \right] \quad \text{for } \frac{m'}{m_1} \leq \hat{r}^{1/2},$$

$$\hat{a}' = 1 \quad \text{for } \frac{m'}{m_1} \geq \hat{r}^{1/2}. \quad (13)$$

A hole that is initially non-rotating ($\hat{r} = 6$) gets spun up to a maximally-rotating state ($\hat{a}' = 1$) after a modest amount of accretion, $m' = m_1\sqrt{6}$. A maximally-rotating hole ($\hat{a} = 1$) gets spun down by retrograde accretion ($\hat{r} = 9$) to $\hat{a}' = 0$ after $m' = m_1\sqrt{3/2}$. A 180° flip of the spin of an extreme-Kerr hole ($\hat{a} = \hat{a}' = 1$) will occur after $m' = 3m_1$.

What is the spin change induced by an accretion disk that is inclined relative to the equatorial plane of the hole? Irrespective of the infalling material’s original angular momentum vector, Lense-Thirring precession will impose axisymmetry close in, with the gas accreting on either prograde or retrograde equatorial orbits. Further out, the disk will be warped where the transition from aligned to misaligned flow occurs (Bardeen & Petterson 1975). This suggests that accretion of material with randomly oriented angular momentum vectors would lead to *spin-down* of a MBH, given the larger LSO of retrograde orbits (Moderski & Sikora 1996).⁶ However, while the material falling into the hole is aligned (or anti-aligned) with it, the torque that aligns the inner disk with the hole must ultimately realign the hole with the outer accretion disk (Rees 1978; Scheuer & Feiler 1996), thus leading to accretion via prograde equatorial orbits. The timescale for this alignment depends on how a warped accretion disk communicates the warp and evolves in time, and is given roughly by (Scheuer & Feiler 1996)

$$t_{\text{align}} \sim 3\hat{a} \left(\frac{m_{\text{BH}}}{\dot{M}} \right) \left(\frac{R_S}{R_w} \right)^{1/2} \left(\frac{\nu_1}{\nu_2} \right) \quad (14)$$

where \dot{M} is the accretion rate onto the hole, R_S is the Schwarzschild radius, R_w is the location of the warp, and ν_1 and ν_2 are the viscosities associated with dissipating motion in and out of the plane of the disk, respectively. For a thin disk of vertical height H , sound speed c_s , and angular velocity Ω , $\nu_2/\nu_1 = (2\alpha^2)^{-1}$ for $1 \gg \alpha > H/R$, where ν_1 is given by the usual Shakura-Sunyaev prescription $\nu_1 = \alpha c_s H = \alpha H^2 \Omega$ (Papaloizou & Pringle 1983).

⁵We have assumed here that the emission of gravitational waves during the plunge phase does not affect the binary energy and angular momentum. This may not be true for nearly equal mass mergers, for which there might not be a well-defined plunge phase (e.g. Pfeiffer, Teukolsky, & Cook 2000).

⁶This argument is similar to that given by HB for why an ensemble of binary coalescences leads to spin-down.

The location of the warp in the disk (R_w) can be estimated by equating the diffusion time of the disk's warp to the timescale for Lense-Thirring precession, which implies (Natarajan & Pringle 1998)

$$\frac{R_w}{R_S} \sim \left(\frac{\hat{a}}{\sqrt{2}\alpha} \right)^{2/3} \left(\frac{R}{H} \right)^{4/3} \left(\frac{\nu_1}{\nu_2} \right)^{2/3}. \quad (15)$$

Substituting equation (15) into equation (14) yields

$$t_{\text{align}} \sim 3 \left(\frac{m_{\text{BH}}}{\dot{M}} \right) \left(\sqrt{2}\hat{a}^2\alpha \right)^{1/3} \left(\frac{\nu_1}{\nu_2} \right)^{2/3} \left(\frac{H}{R} \right)^{2/3}. \quad (16)$$

Equation (16) shows that, for thin accretion disks with $H \ll R$, the alignment time is much less than the timescale for the mass of the hole to increase via accretion (using α -disk models, Natarajan & Pringle 1998 and Natarajan & Armitage 1999 estimate $t_{\text{align}} \sim 10^5 - 10^6$ yrs for accretion near the Eddington limit). As a result, the hole will align itself with the outer disk before it accretes much mass. This implies that most of the mass accreted by the hole will act to spin it up (i.e., the magnitude of the spin increases in time), even if the direction of the spin axis changes in time. This is true unless the angular momentum of the inflowing material changes significantly on a timescale $\ll t_{\text{align}}$.

If the mass supply rate to a MBH is super-Eddington, accretion proceeds via a radiation pressure supported thick disk with $H \sim R$ (e.g., Begelman & Meier 1982). Equations (15) and (16) show that in this case $R_w \sim R_S$ and alignment is relatively inefficient, occurring on a timescale comparable to the timescale for changes in the hole's mass (the Salpeter time). It is possible that much of the growth of MBHs at high redshift occurs via a radiation pressure supported thick disk, rather than a thin accretion disk.⁷ In fact, it would be surprising if the mass supply rate were precisely \sim Eddington (required for a thin disk) during the entire growth of MBHs. It is perhaps more likely that the mass supply rate is initially larger in the dense gas-rich environments of high redshift galaxies and then decreases with time as the galaxy is assembled.

In the extreme case in which alignment is always relatively inefficient, as would be expected for accretion via a thick disk, we can generalize equations (7), (8), and (9) to determine the angular momentum evolution under gas accretion as follows:

$$dm = dm_0 \hat{E}(\hat{a}_1, \mu), \quad (17)$$

$$dS_z = m_1 dm_0 \hat{L}_z(\hat{a}_1, \mu), \quad (18)$$

$$dS_{\perp} = m_1 dm_0 \hat{L}_z(\hat{a}_1, \mu) \sqrt{\mu^{-2} - 1}. \quad (19)$$

This equation can be integrated numerically to yield the final orientation and magnitude of the hole spin after each accretion episode, for a given inclination.

Finally, we note that Thorne (1974) showed that the radiation emitted by the disk and swallowed by the hole produces a counteracting torque, which prevents spin up beyond $\hat{a}' = 0.998$. Magnetic fields connecting material in the disk and the plunging region may further reduce

the equilibrium spin by transporting angular momentum outward. Fully relativistic magnetohydrodynamic simulations for a series of thick accretion disk models show that spin equilibrium is reached at $\hat{a}' \approx 0.93$ (Gammie, Shapiro, & McKinney 2004). For simplicity, we will assume in the following that a MBH may be spun up to a maximum equilibrium value of $\hat{a}' = 0.998$.

5. MBH SPIN DISTRIBUTION AND EVOLUTION

The combination of a halo merger tree and our semi-analytical scheme to treat the growth of MBHs and their dynamics is a powerful tool for tracking the evolution of MBH spins with cosmic time. In our merger tree, MBHs that undergo an accretion episode typically increase their mass by about one e-folding. This is required in order to account for the local mass density of MBHs with growth solely during major mergers. The distribution of fractional changes in hole mass from gas accretion is shown in Figure 4 for different redshift intervals. Note how, at all epochs, a significant fraction of accretion events leads to $\Delta m/m_1 \gtrsim 2-3$: these individual episodes will produce rapidly-rotating holes independent of the initial spin.

To bracket the uncertainties and explore various scenarios we have run different sets of Monte Carlo realizations. Our “fiducial” model assumes seed holes are born with an initial spin of $\hat{a} = 0.6$ (Fryer, Woosley, & Heger 2002). The evolution (both in magnitude and orientation) of MBH spins is driven by gas accretion and black hole binary coalescences. Whenever a binary forms, the angle of inclination of the smaller hole relative to the equatorial plane is chosen randomly from an isotropic distribution. We assume that during a major merger the gas accretes via a thin disk; efficient alignment between the hole and the outer disk implies that most of the mass is accreted in prograde equatorial orbits (§4).

Figure 5 shows the ensuing spin distribution of MBHs at different epochs. The left panel depicts the effect of binary coalescences alone on the spin distribution. At late epochs binaries with small mass ratios are common (Fig. 1), as some less massive holes that were wandering in galaxy halos at high redshift – with an orbital decay timescale comparable to the Hubble time – finally find their way to galaxy centers. In addition, our assumption that, following a major merger between halos, a new accretion episode is triggered only on the more massive hole, probably somewhat underpredicts the mass ratio of coalescing holes. A more realistic model in which both holes accrete would lead to somewhat larger mass ratios, though this effect is likely to be mild given that the mass accreted per merger is comparable to the mass of the pre-existing hole (Fig. 4).

Figure 5 shows that repeated captures of smaller holes cause a spread both towards $\hat{a} > 0.6$ (spin up) and $\hat{a} < 0.6$ (spin down) in $N(\hat{a})$. The relatively flat distribution of $N(q)$ for captures in hierarchical models (Fig. 1) implies that neither spin-up nor spin-down is particularly favored. The holes random walk around the initial “seed” value, and the spin distribution retains memory of the initial rotation black holes are endowed with at birth. For comparison, we also show a case in which seed holes are

⁷If the mass supply rate is super-Eddington, most of the inflowing gas is likely driven away in a radiation-pressure driven outflow, limiting the accretion rate onto the hole to \sim the Eddington rate (e.g., Shakura & Sunyaev 1973; Blandford & Begelman 2004). Thus accretion via a geometrically thick disk may still be compatible with the mean accretion efficiency of $\sim 10\%$ inferred by, e.g., Yu & Tremaine (2002).

born *non-spinning* instead (dashed histogram in the left panel). Again, at all redshifts, the spin distribution remains peaked around $\hat{a} = 0$. The right panel in Figure 5 includes spin changes both by captures and by gas accretion. Gas accretion dominates the spin evolution over coalescences (the initial mass in seed holes is a tiny fraction of the mass density observed today). At all epochs, nearly all MBHs are spun-up by accretion to $\hat{a} \approx 1$.

Figure 6 shows the spin evolution history of two MBHs that end up in massive halos with $M_h = 10^{12} M_\odot$ at $z = 0$. Note how gas accretion (lower panel) efficiently spins the holes up, while binary coalescences lead to both spin-up and spin-down. Figures 7 and 8 explore the uncertainties introduced by some of our assumptions. Figure 7 shows the evolution of the spin under binary coalescences alone, comparing two examples where we placed seed holes in 3σ and 3.5σ peaks at high redshift. The former example has a total of ~ 50 times more seed holes, leading to ~ 10 times more binary coalescences;⁸ the total mass in seed holes is now a larger fraction of the mass density in MBHs observed today. Despite the significant increase in the number of binary coalescences, the spin evolution is reasonably similar in the two examples. The most notable difference is that there are fewer rapidly rotating holes at low redshift in the case with more seed holes, because of spin-down by capture of smaller companions at late times (see Fig. 1). The overall effect is, however, rather mild, and the spin distribution still retains significant memory of the initial conditions; binary coalescences alone thus do not lead to a significant systematic spin-up or spin-down of MBHs.

Figure 8 shows an example where alignment of the hole and the outer disk is inefficient, as would be expected if accretion is via a geometrically thick disk (§4). We assume that the initial orientation between the black hole’s spin and the accretion disk rotation axis is random, and integrate equations (17)-(19) for every accretion episode, i.e. we treat binary coalescences and gas accretion in a similar way. This would seem to favor spin-down of the MBHs, and yet even in this case most of the holes are rotating quite rapidly at all epochs. The reason is that the accreted mass is typically larger than the hole’s mass (Fig. 4). Most individual accretion episodes thus produce rapidly-rotating holes independent of the initial spin.

6. SUMMARY AND DISCUSSION

We have computed the expected distribution of MBH spins and its evolution with cosmic time in the context of hierarchical structure formation theories. A subset of the current authors have previously described models for the birth, growth, and dynamics of MBHs that traces their build-up far up the dark halo “merger tree” in a Λ CDM cosmology (see, e.g., Volonteri et al. 2003). Here we have extended this work to follow the combined effects of black hole-black hole coalescences and accretion from a gaseous disk on the magnitude and orientation of MBH spins.

We find that binary coalescences cause no significant systematic spin-up or spin-down of MBHs: because of the relatively flat distribution of MBH binary mass ratios in hierarchical models (Fig. 1), the holes random-walk around

the spin parameter they are endowed with at birth, and the $N(\hat{a})$ distribution retains significant memory of the initial rotation of “seed” holes (Figs. 5 and 7).

In our models, accretion, not binary coalescences, dominates the spin evolution of MBHs. Accretion can lead to efficient spin-up of MBHs even if the angular momentum of the inflowing material varies in time. This is because, for a thin accretion disk, the hole is aligned with the outer disk on a timescale that is much shorter than the Salpeter time (eq. 16; Natarajan & Pringle 1998), leading to accretion via prograde equatorial orbits. As a result, most of the mass accreted by the hole acts to spin it up, even if the orientation of the spin axis changes in time. For a geometrically thick disk, alignment of the hole with the outer disk is much less efficient, occurring on a timescale comparable to the Salpeter time. In this case we still find that most holes are rotating rapidly (Fig. 8). This is because, in any model in which MBH growth is triggered by major mergers, every accretion episode must typically increase a hole’s mass by about one e-folding to account for the local MBH mass density and the $m_{\text{BH}} - \sigma_*$ relation. Most individual accretion episodes thus produce rapidly-rotating holes independent of the initial spin.

Under the combined effects of accretion and binary coalescences, we find that the spin distribution is heavily skewed towards fast-rotating Kerr holes, is already in place at early epochs, and does not change significantly below redshift 5. As shown in Figure 9, about 70% of all MBHs are maximally rotating and have mass-to-energy conversion efficiencies approaching 30%. Note that if the equilibrium spin attained by accreting MBHs is lower than the value of $\hat{a} = 0.998$ used here, as in the thick disk MHD simulations of Gammie et al. (2004) where $\hat{a} \approx 0.93$, then the accretion efficiency will be lower as well, $\approx 17\%$ for $\hat{a} \approx 0.93$. Even in the conservative case where accretion is via a geometrically thick disk (and hence the spin/disk alignment is relatively inefficient) and the initial orientation between the hole’s spin and the disk rotation axis is assumed to be random, we find that most MBHs rotate rapidly with spin parameters $\hat{a} > 0.8$ and accretion efficiencies $\epsilon > 12\%$. As recently shown by Yu & Tremaine (2002), Elvis, Risaliti, & Zamorani (2002), and Marconi et al. (2004), a direct comparison between the local MBH mass density and the mass density accreted by luminous quasars shows that quasars have a mass-to-energy conversion efficiency $\epsilon \gtrsim 0.1$ (a simple and elegant argument originally provided by Soltan 1982). This high average accretion efficiency may suggest rapidly rotating Kerr holes, in agreement with our findings.

In our models, there is a weak trend for the most massive and the least massive holes to have slightly lower spin parameters (efficiencies), the former because they experience more binary coalescences during their lifetime, and the latter because they experience a smaller number of accretion episodes.

One way to avoid rapid rotation and produce slowly rotating holes is to assume “chaotic feeding” in which small amounts of material, with $\Delta m \ll m_{\text{BH}}$, are swallowed by the hole in successive accretion episodes with random

⁸The nonlinear increase in the number of binary coalescences in going from 3.5 to 3 σ peaks is due to several factors: (1) there are a larger number of halo minor mergers that never form MBH binaries because of the long dynamical friction timescales, and (2) a larger number of holes are ejected from their host galaxies by triple interactions and gravitational recoil.

orientations (e.g., Moderski and Sikora 1996). The constraints on such a model appear, however, to be stringent. Specifically, for a thin disk the angular momentum of the inflowing material must vary on a timescale $\lesssim t_{\text{align}} \ll t_{\text{Salpeter}}$. Otherwise alignment of the hole with the outer disk ensures that most of the mass accreted by the hole spins it up. The required timescale for angular momentum reversals is much shorter than that expected in merger-initiated nuclear activity, but could in principle be provided by (say) accretion of molecular clouds on random orbits.

In this context, an issue which must be investigated further is the alignment of the BH spin axis and the angular momentum axis of the outer disk when the initial angle is more than 90 degrees. In this case the inner disk ends up “anti-aligned” instead of “aligned”; to fully align the hole with the outer disk requires the inner disk to “flip” by 180 degrees. If the timescale for alignment is as short as we have assumed for the thin disk geometry, then the initial period of “anti-alignment” is probably not important, but if the timescale is of order the Salpeter timescale

successive accretion events could cancel out.

To explain the dichotomy between radio-quiet and radio-loud quasars, Wilson & Colbert (1995) suggested that in all radio-quiet quasars the MBH is slowly rotating. Since most holes rotate rapidly in our models, our results suggest instead that the spin of a MBH is not a necessary and sufficient condition for producing a radio-loud quasar. Independent evidence for this conclusion comes from observations of X-ray binaries, where jets are observed to be present only in the hard/low X-ray spectral state, but not in the soft/high state (Fender 2001). This favors a model in which the mode of accretion, perhaps together with the spin, determines the radio loudness of an accreting black hole (e.g., Rees et al. 1982; Meier 2001).

Support for this work was provided by NASA grants NAG5-11513 and NNG04GK85G, and by NSF grant AST-0205738 (PM). EQ is supported in part by NSF grant AST 0206006, NASA grant NAG5-12043, an Alfred P. Sloan Fellowship, and the David and Lucile Packard Foundation.

REFERENCES

- Armitage, P. J., & Natarajan, P. 2002, *ApJ*, 567, L9
 Bardeen, J. M. 1970, *Nature*, 226, 64
 Bardeen, J. M., & Petterson, J. A. 1975, *ApJ*, 195, L65
 Bardeen, J. M., Press, W. H., & Teukolsky, S. A. 1972, *ApJ*, 178, 347
 Begelman, M. C., Blandford, R. D., & Rees, M. J. 1980, *Nature*, 287, 307
 Begelman, M. C. & Meier, D. L., 1982, *ApJ*, 253, 873
 Blandford, R. D., & Begelman, M. C. 2004, *MNRAS*, 349, 68
 Blandford, R. D., & Znajek, R. L. 1977, *MNRAS*, 179, 433
 Elvis, M., Risaliti, G., & Zamorani, G. 2002, *ApJ*, 565, L75
 Escala, A., Larson, R. B., Coppi, P. S., & Mardones, D. 2004, *ApJ*, 607, 765
 Fender, R. P. 2001, *MNRAS*, 322, 31
 Ferrarese, L. 2002, *ApJ*, 578, 90
 Ferrarese, L., & Merritt, D. 2000, *ApJ*, 539, L9
 Fryer, C. L., Woosley, S. E., & Heger, A. 2001, *ApJ*, 550, 372
 Gammie, C. F., Shapiro, S. L., & McKinney, J. C. 2004, *ApJ*, 602, 312
 Gebhardt, K., et al. 2000, *ApJ*, 543, L5
 Häring, N., & Rix, H.-W. 2004, *ApJ*, 604, L89
 Hughes, S. A., & Blandford, R. D. 2003, *ApJ*, 585, L101 (HB)
 Krolik, J. H., Hawley, J. F., & Shigenobu H. 2004, *ApJ*, submitted (astro-ph/0409231)
 Madau, P., & Rees, M. J. 2001, *ApJ*, 551, L27
 Marconi, A., Risaliti, G., Gilli, R., Hunt, L. K., Maiolino, R., & Salvati, M. 2004, *MNRAS*, 351, 169
 Meier, D. L. 2001, *ApJ*, 548, L9
 Merritt, D., & Ekers, R. D. 2002, *Science*, 297, 1310
 Moderski, R., & Sikora, M. 1996, *A&AS*, 120, 591
 Natarajan, P. & Armitage, P. J., 1999, *MNRAS*, 309, 961
 Natarajan, P., & Pringle, J. E. 1998, *ApJ*, 506, L97
 Navarro, J. F., Frenk, C. S., & White, S. D. M. 1997, *ApJ*, 490, 493
 Papaloizou, J. C. B. & Pringle, J. E., 1983, *MNRAS*, 202, 1181
 Pfeiffer, H. P., Teukolsky, S. A., & Cook, G. B. 2000, *PhRvD*, 62, 104018
 Quinlan, G. D. 1996, *NewA*, 1, 35
 Rees, M. J. 1978, *Nature*, 275, 516
 Rees, M. J. 1984, *ARA&A*, 22, 471
 Rees, M. J., Phinney, E. S., Begelman, M. C., & Blandford, R. D. 1982, *Nature*, 295, 17
 Richstone, D., et al. 1998, *Nature*, 395, 14
 Saslaw, W. C., Valtonen, M. J., & Aarseth, S. J. 1974, *ApJ*, 190, 253
 Scheuer, P. A. G., & Feiler, R. 1996, *MNRAS*, 282, 291
 Shakura, N. I., & Sunyaev, R. A. 1973, *A&A*, 24, 337
 Soltan, A. 1982, *MNRAS*, 200, 115
 Thorne, K. S. 1974, *ApJ*, 191, 507
 Volonteri, M., Haardt, F., & Madau, P. 2003, *ApJ*, 582, 559
 Volonteri, M., Madau, P., & Haardt, F. 2003, *ApJ*, 593, 661
 Wilson, A. S., & Colbert, E. J. M. 1995, *ApJ*, 438, 62
 Yu, Q. 2002, *MNRAS*, 331, 935
 Yu, Q., & Tremaine, S. 2002, *MNRAS*, 335, 965

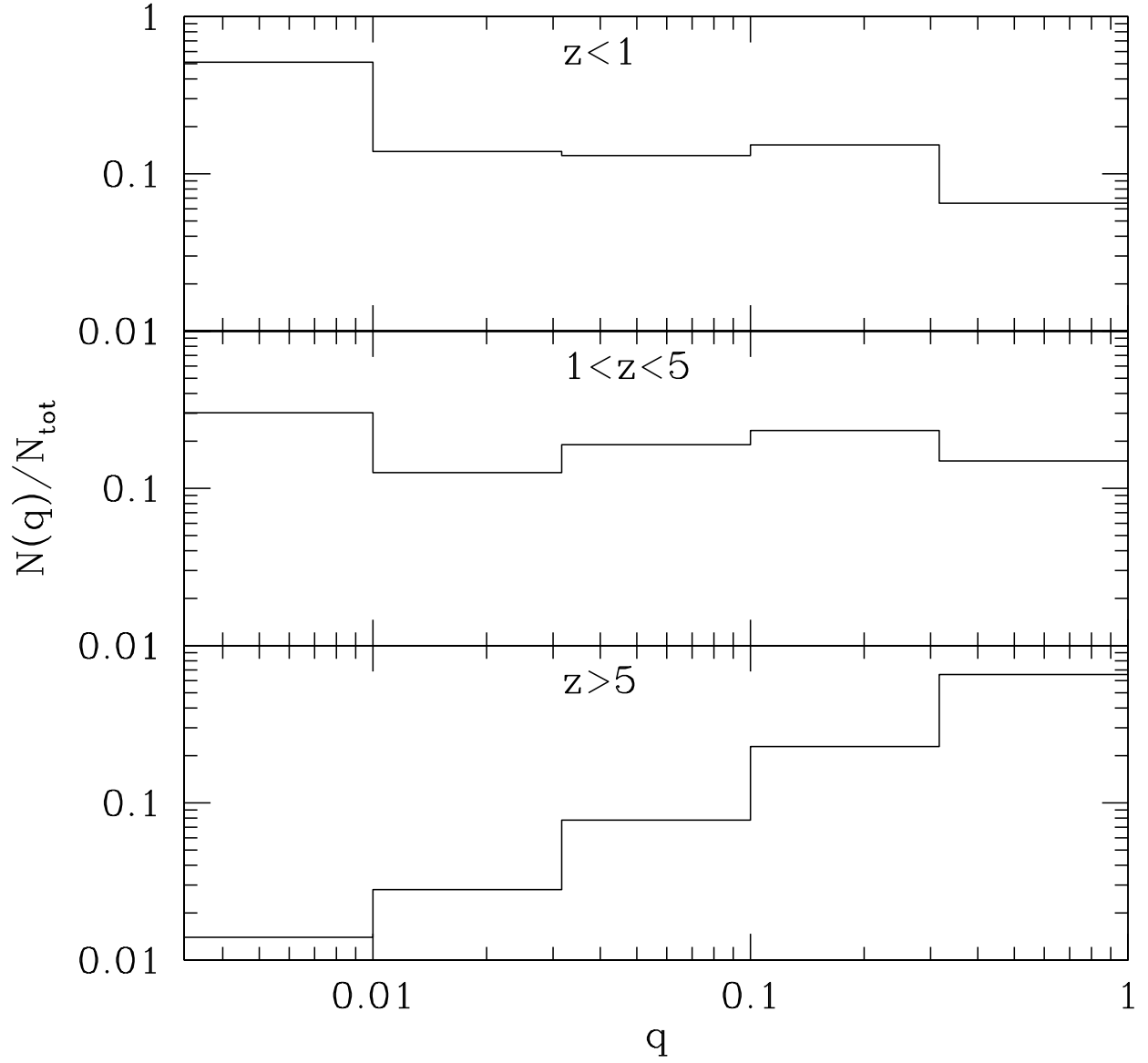


FIG. 1.— Normalized distribution of mass ratios of coalescing MBH binaries at three different epochs. Note that at low redshift MBHs typically capture much smaller companions.

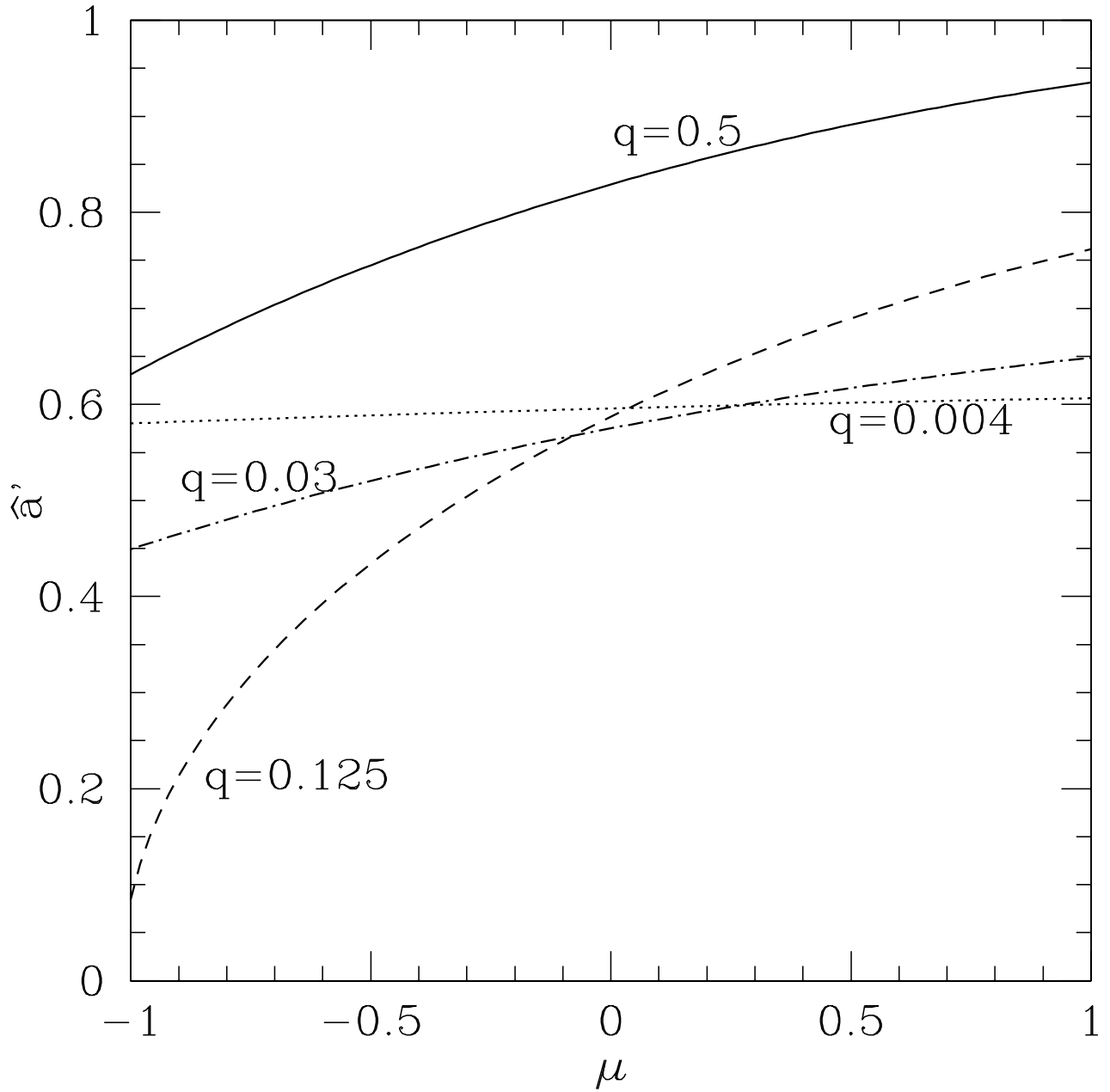


FIG. 2.— Final spin \hat{a}' of the remnant MBH as a function of inclination angle $\mu = \cos \theta$, for different binary mass ratios $q = m_2/m_1$. Before coalescence, the larger hole has spin $\hat{a}_1 = 0.6$. The remnant is typically spun down for $q < 0.125$, and is spun up otherwise.

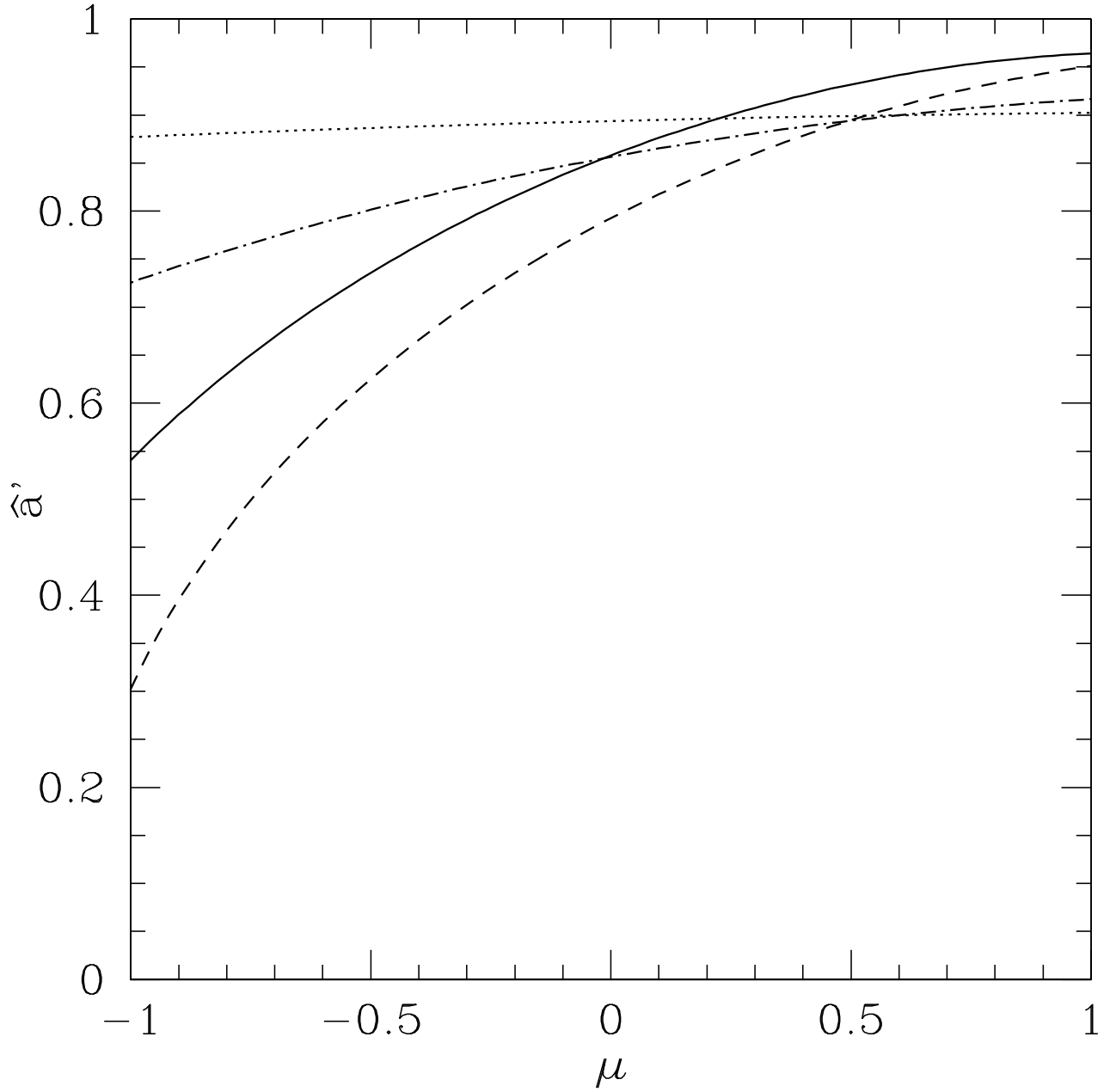


FIG. 3.— Same as Fig. 2, but with $\hat{a}_1 = 0.9$. For most of the parameter space, the remnant MBH is spun down.

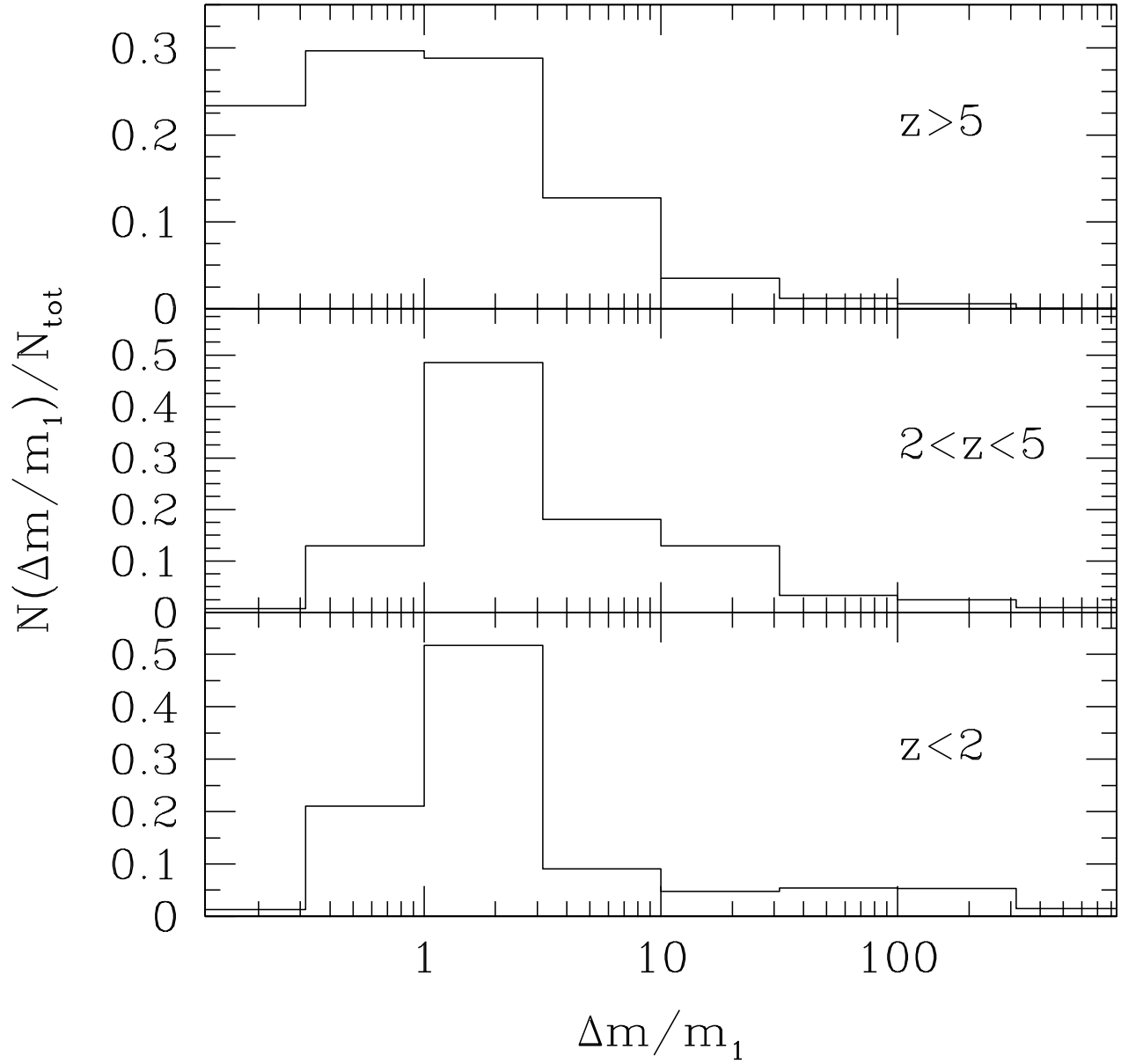


FIG. 4.— Distribution of fractional changes in the mass of a MBH as a result of the accretion of material after a major halo merger. Different redshift intervals are shown.

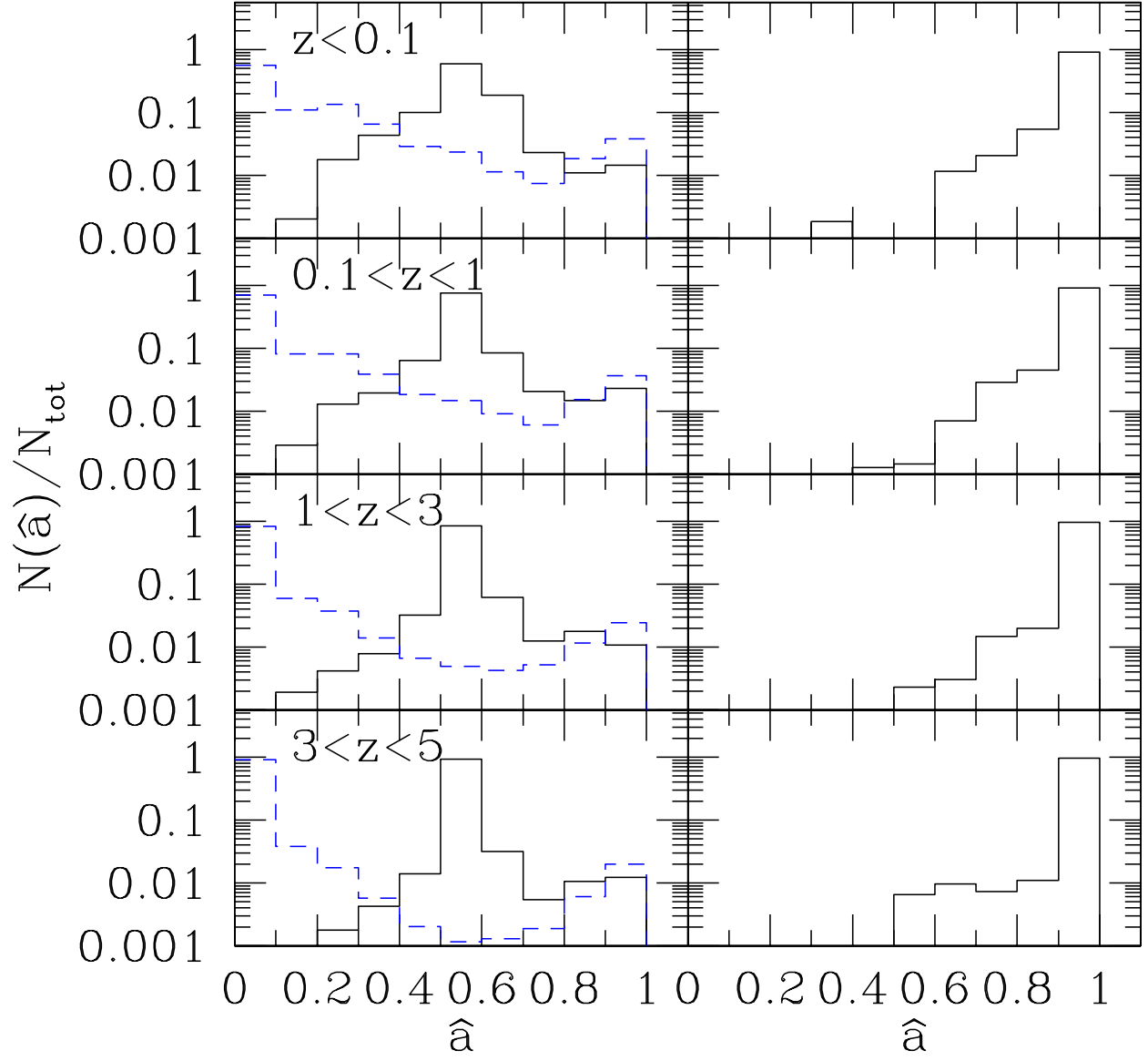


FIG. 5.— Distribution of MBH spins in different redshift intervals. *Left panel:* effect of black hole binary coalescences only. *Solid histogram:* “seed” holes are born with $\hat{a} = 0.6$. *Dashed histogram:* “seed” holes are born non-spinning. *Right panel:* spin distribution from binary coalescences and gas accretion. “Seed” holes are born with $\hat{a} = 0.6$, and are efficiently spun up by accretion via a thin disk.

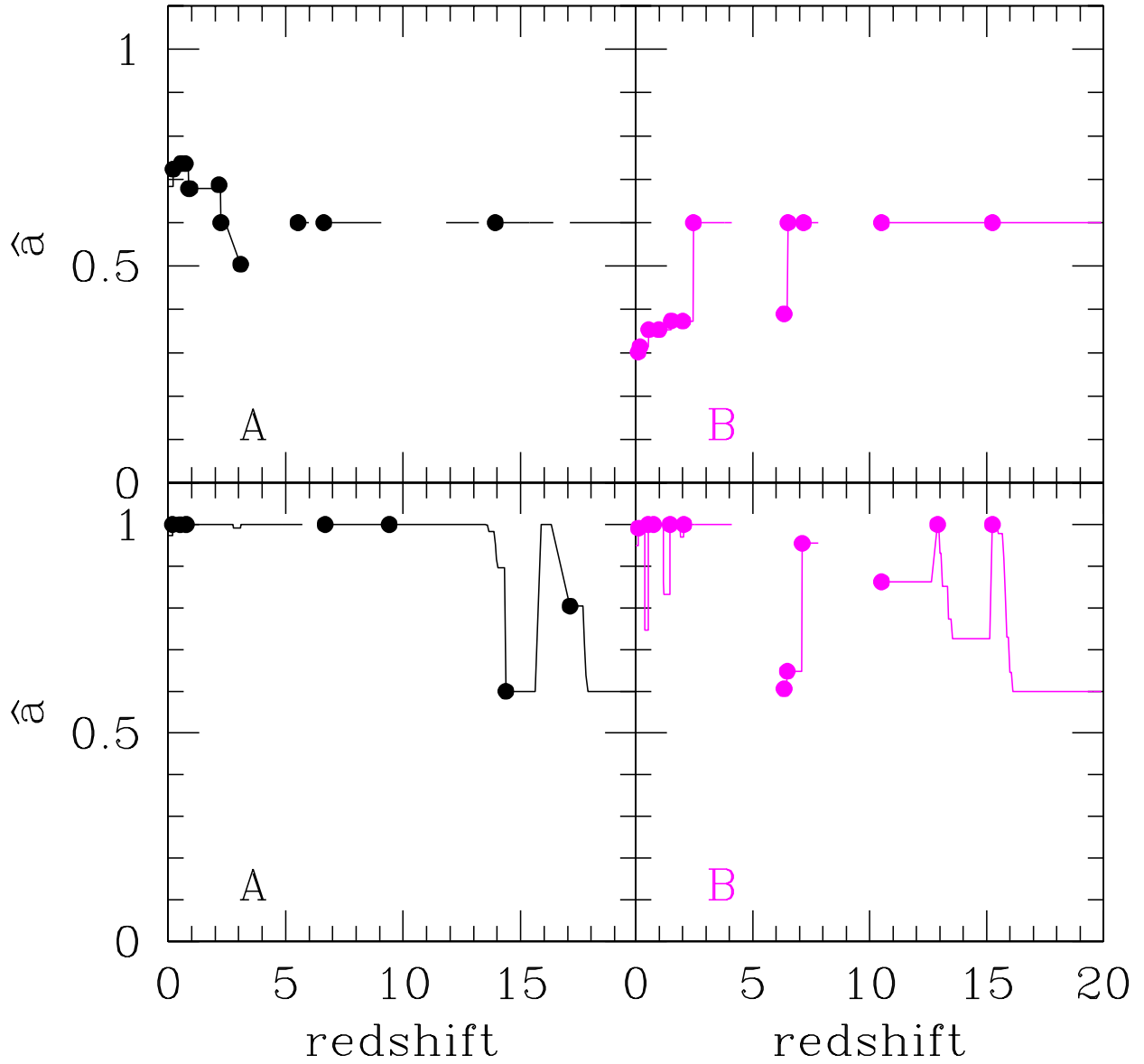


FIG. 6.— The spin evolution of two MBHs, “A” (*left panels*) and “B” (*right panels*), that end up in massive halos with $M_h = 10^{12} M_\odot$ at $z = 0$. The initial spin of “seed” holes is $\hat{a} = 0.6$. *Upper panel:* the spin of black holes is modified by binary coalescences only. *Lower panel:* the spin evolution is driven by black hole binary coalescences and gas accretion. The dots mark the epoch when two MBHs coalesce. Note the intermittent times when halos are devoid of a central MBH, after an ejection due to radiation recoil. The halo (re)gains a central MBH after the original one falls back in or the halo experiences a merger with another halo, whose MBH becomes the central hole of the newly formed galactic system.

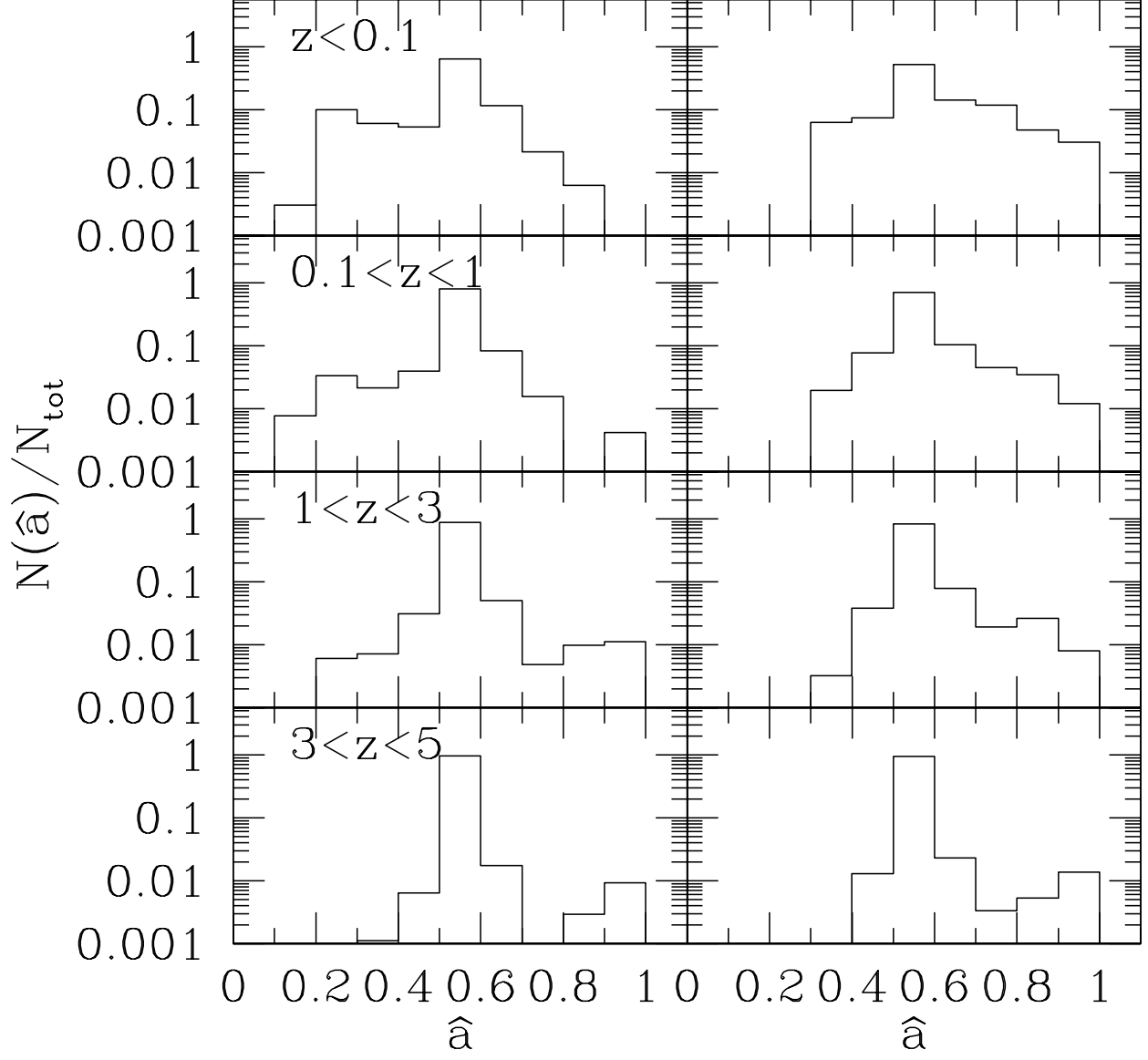


FIG. 7.— The spin distribution for MBHs that end up in massive halos with $M_h = 10^{12} M_\odot$ at $z = 0$. Spins evolve under by binary coalescences alone. *Left panel:* “seed” holes are placed in 3σ peaks at $z = 20$. *Right panel:* “seed” holes are placed in 3.5σ peaks at $z = 20$. In both cases black holes are born with $\hat{a} = 0.6$. The model in the left panel has ≈ 10 times more coalescences than that in the right panel, but the resulting spin distributions are quite similar.

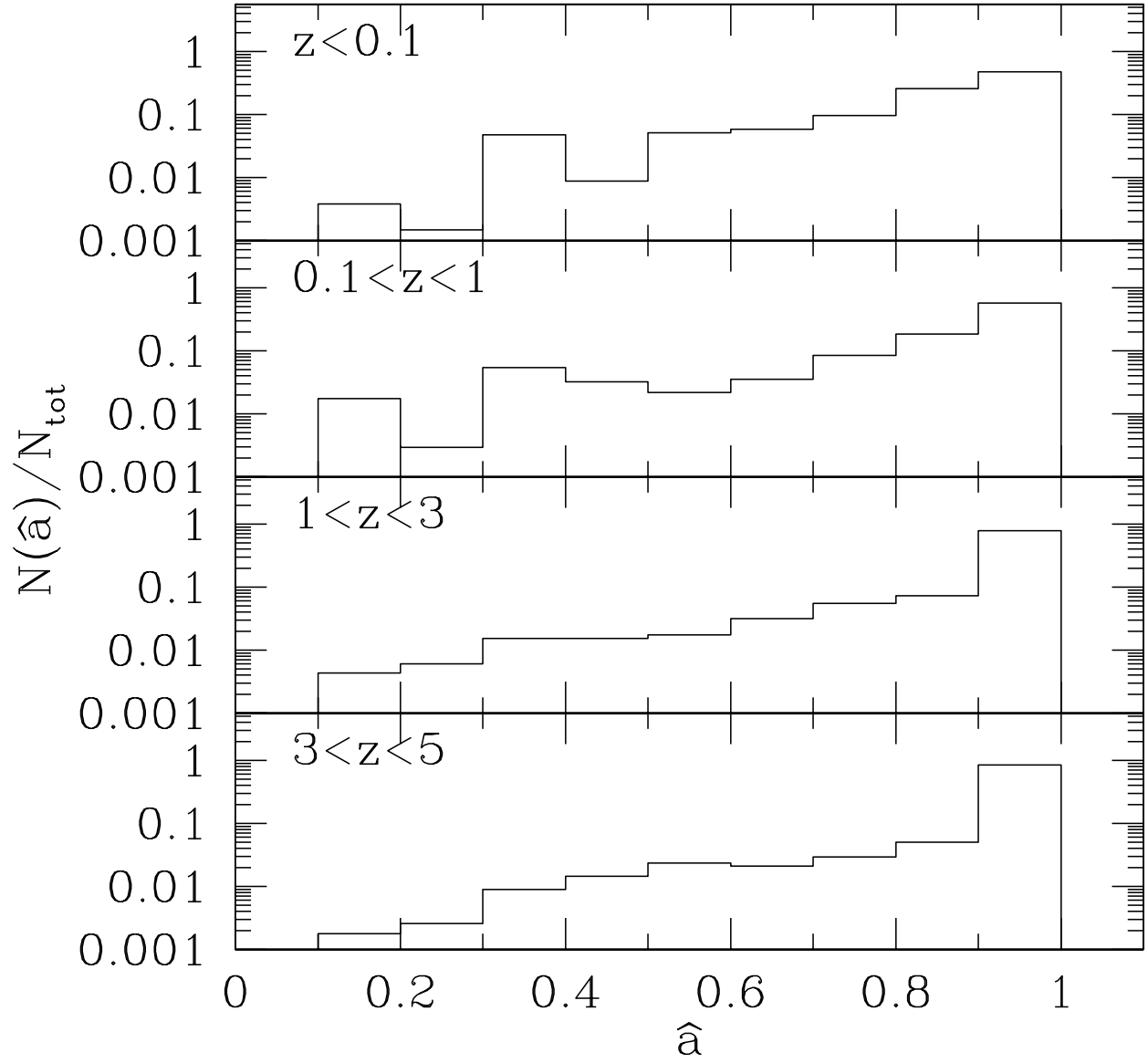


FIG. 8.— Distribution of MBH spins in different redshift intervals. The spin is modified by binary coalescences and by accretion; alignment of the hole and the outer disk is assumed to be inefficient, as would be expected for accretion via a geometrically thick disk. The initial orientation between hole's spin and disk angular momentum is assumed to be random.

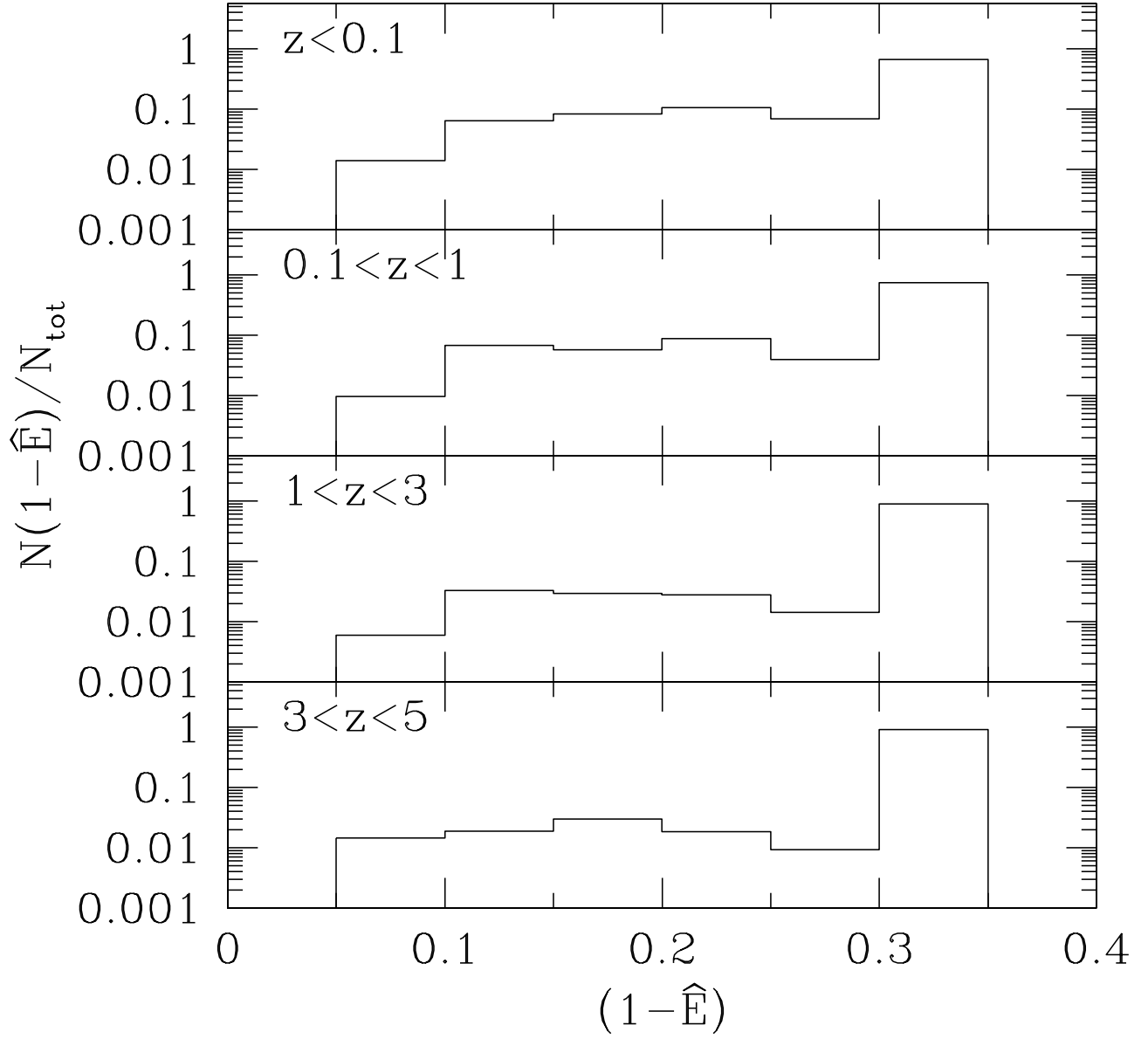


FIG. 9.— Distribution of accretion efficiencies, $\epsilon \equiv 1 - \hat{E}$, in different redshift intervals (assuming that the energy radiated is the binding energy at the LSO). The spin distribution from binary coalescences and gas accretion has been calculated assuming the holes accrete via a thin disk on prograde equatorial orbits.